

CONSTRAINING DECAYING DARK MATTER WITH THE EFFECTIVE FIELD THEORY OF LARGE-SCALE STRUCTURE

THÉO SIMON

*Laboratoire Univers & Particules de Montpellier (LUPM), CNRS & Université de Montpellier
(UMR-5299), Place Eugène Bataillon, F-34095 Montpellier Cedex 05, France*

I present the first constraints on decaying cold dark matter (DCDM) models thanks to the effective field theory of large-scale structure (EFTofLSS) applied to BOSS-DR12 data. I consider two phenomenological models of DCDM: i) a model where a fraction f_{dcdm} of cold dark matter (CDM) decays into dark radiation (DR) with a lifetime τ ; ii) a model (recently suggested as a potential resolution to the S_8 tension) where all the CDM decays with a lifetime τ into DR and a massive warm dark matter (WDM) particle, with a fraction ε of the CDM rest mass energy transferred to the DR. I discuss the implications of the EFTofLSS constraints for the DCDM model suggested to resolve the S_8 tension.

1 Introduction

The core cosmological model, known as the Λ cold dark matter (Λ CDM) model, delivers an exceptional explanation for a broad variety of early and late Universe data. However, as the accuracy of measurements has increased over the past few years, some intriguing discrepancies have emerged within this model: for instance, the “ S_8 tension”¹ corresponds to a mismatch of the value of the amplitude of the local matter fluctuations (typically parameterized as S_8) between its prediction by the Λ CDM model from the CMB data^{2,3} on the one hand, and its direct and local determination on the other hand^{4,5,6,7} (the latter being weaker than the former). The S_8 parameter is defined as $S_8 = \sigma_8 \sqrt{\Omega_m/0.3}$, where Ω_m is the current total matter abundance, and σ_8 is the root mean square of matter fluctuations on a $8 h^{-1}\text{Mpc}$ scale (with $h = H_0/(100 \text{ km/s/Mpc})$). This tension could be the first indication of new features in the dark components which would cause a decrease in the power spectrum at scales $k \sim 0.1 - 1 \text{ Mpc}/h$. We present here⁸ two decaying cold dark matter models that have the ability to lead to such a suppression.^{9,10,11,12,13,14,15,16,17,18,19,20}

Here, we go beyond previous works by making use of the effective field theory of large-scale structure (EFTofLSS)^{21,22,23,24} to describe the mildly non-linear regime of the galaxy clustering power spectrum and derive improved constraints thanks to the EFTofLSS applied to BOSS data^{25,26} (EFTofBOSS). Despite some precautions to be taken in the interpretation of the results,²⁷ the EFTofBOSS data have been shown to allow for the determination of the Λ CDM parameters^{28,29,30,31,32,33,34,27,35,36} at a precision higher than that from conventional BAO and redshift space distortions (denoted as “BOSS BAO/ $f\sigma_8$ ”), as well as to provide interesting constraints on models beyond Λ CDM.^{30,37,38,39,40,41,42,43,44,45,46,47,8,48,49,50}

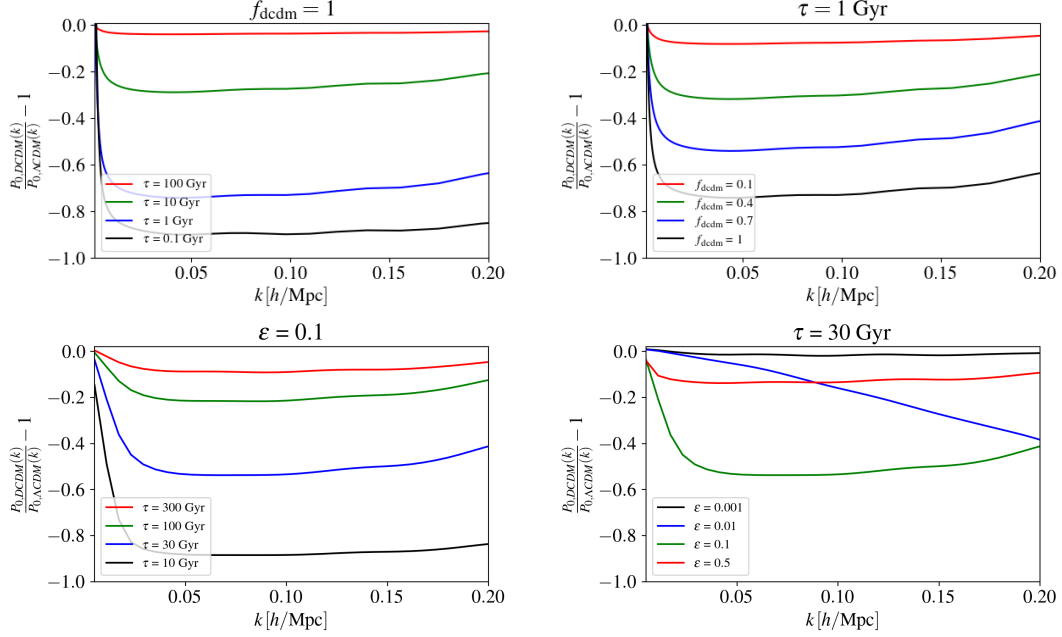


Figure 1 – *Upper* - Residuals (with respect to the Λ CDM model at $z = 0$) of the monopole of the DCDM \rightarrow DR galaxy power spectrum for several values of f_{dcdm} and τ . *Lower* - The same applies to the DCDM \rightarrow WDM+DR model with several values of τ and ε .

2 Constraints on the DCDM \rightarrow DR model

2.1 Presentation of the model

In the first model we consider,¹³ the CDM sector is partially composed of an unstable particle (denoted as DCDM) that decays into a non-interacting relativistic particle (denoted as DR). The rest of the DM is considered stable and we refer to it as the standard CDM. In addition to the standard six Λ CDM parameters, there are two free parameters describing the lifetime of DCDM τ (or equivalently the decay width $\Gamma = \tau^{-1}$), as well as the fraction of DCDM to total dark matter at the initial time $a_{\text{ini}} \rightarrow 0$: $f_{\text{dcdm}} \equiv \omega_{\text{dcdm}}(a_{\text{ini}})/\omega_{\text{tot, dm}}(a_{\text{ini}})$, with $\omega_{\text{tot, dm}} \equiv \omega_{\text{dcdm}} + \omega_{\text{cdm}}$. With these definitions, in the limit of large τ and/or small f_{dcdm} , one recovers the Λ CDM model. The evolution of the homogeneous energy densities of the DCDM and DR is given by¹³:

$$\dot{\bar{\rho}}_{\text{dcdm}} + 3\mathcal{H}\bar{\rho}_{\text{dcdm}} = -a\Gamma\bar{\rho}_{\text{dcdm}} \quad ; \quad \dot{\bar{\rho}}_{\text{dr}} + 4\mathcal{H}\bar{\rho}_{\text{dr}} = a\Gamma\bar{\rho}_{\text{dcdm}}, \quad (1)$$

where \mathcal{H} is the conformal Hubble parameter.

To describe the evolution of the linearly perturbed universe, we consider the usual synchronous gauge, where the frame co-moving with the DCDM (and CDM) fluid. Since we consider a homogeneous and isotropic decay, the energy density perturbation of the DCDM component, $\delta_{\text{dcdm}} \equiv \rho_{\text{dcdm}}/\bar{\rho}_{\text{dcdm}} - 1$, follows the same evolution as standard CDM. Consequently, the specific effects of the DCDM \rightarrow DR model occur at the background level (since the effect of the daughter particles is minor).

In the upper panel of Fig. 1, we represent the residuals of the monopole of the galaxy power spectrum for several values of f_{dcdm} and τ to isolate their cosmological effects: as expected, deviations with respect to Λ CDM increases as τ decreases and/or f_{dcdm} increases. This deviation takes the appearance of a power suppression due to two main reasons.¹³ First, the decay of DCDM decreases the duration of the matter dominated era (and at fix h , a smaller Ω_m /larger Ω_Λ), implying a shift of the power spectrum towards large scales, *i.e.* towards small wavenumbers. Second, DCDM models involve a larger ratio of $\omega_b/\omega_{\text{cdm}}$ compared to the Λ CDM model due to the decay. Both effects manifests as a strong suppression of the small-scale power spec-

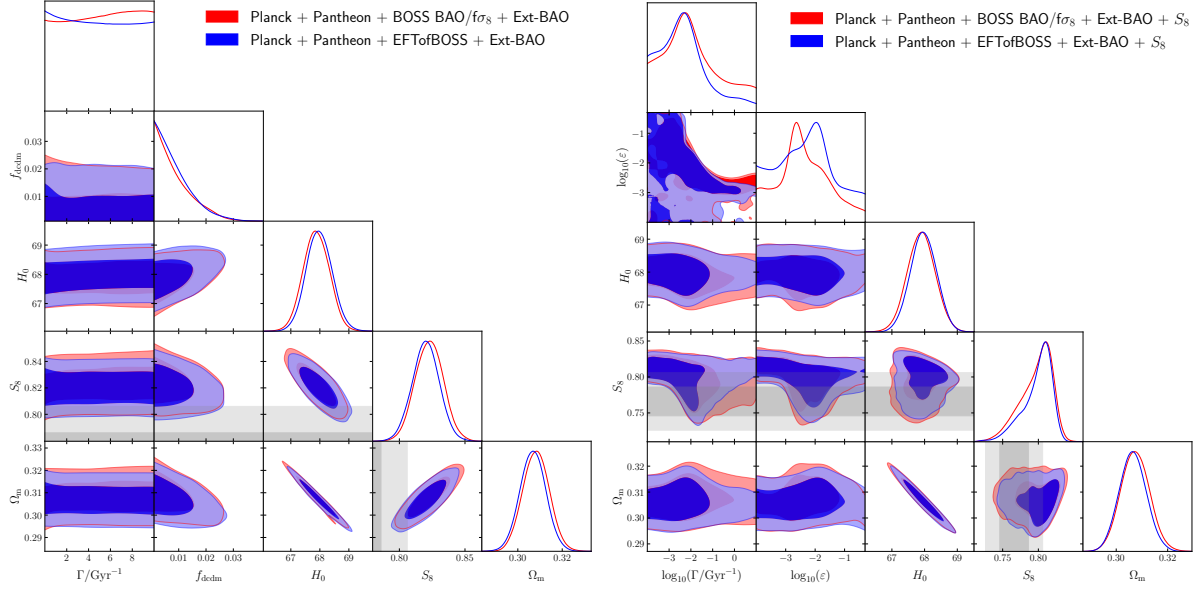


Figure 2 – *Left* - 2D posterior distributions of the DCDM \rightarrow DR model with and without the EFTofBOSS dataset. The gray shaded bands refer to the joint S_8 measurement from KiDS-1000 + BOSS + 2dFLens. *Right* - 2D posterior distributions of the DCDM \rightarrow WDM+DR model with and without the EFTofBOSS dataset.

trum, and the latter effect leads to an additional modulation of the BAO amplitude visible as wiggles in the upper panel of Fig. 1.

2.2 EFTofLSS Constraints on the DCDM \rightarrow DR model

In the left panel of Fig. 2, we display the 1D and 2D posteriors of the reconstructed parameters for the DCDM \rightarrow DR model with and without the EFTofBOSS dataset. When we do not take into account the data from EFTofBOSS, we include the standard RSD information, denoted as “BOSS BAO/ $f\sigma_8$ ”. In these analysis, we always take into account data from *Planck*² (namely the CMB power spectra as well as the gravitational lensing potential), Pantheon⁵¹ and Ext-BAO^{52,53,54,55} (which corresponds to measurements using the BAO information without EFT treatment).

One can see that the inclusion of the EFTofBOSS data does not improve the constraints on this model with respect to the standard RSD information. However, while τ is unconstrained, we obtain an interesting 95 % C.L constraint on the DCDM fraction : $f_{\text{dcdm}} < 0.0216$. We perform a second analysis⁸ where we set $f_{\text{dcdm}} = 1$ in order to derive a lower constraint on τ . We obtain, at 95 % C.L., $\tau > 249.6$ Gyr.

Finally, we show⁸ that when adding a S_8 prior from the KIDS-1000 cosmic shear measurement, the $\Delta\chi^2$ with respect to Λ CDM is still compatible with zero. We conclude (as in past studies) that this model does not resolve the S_8 tension. This is because the suppression of the power spectrum (which could allow us to resolve the S_8 tension) is mainly due to a background effect, through the decrease of Ω_m . This latter parameter is however well constrained by the different data we have taken into account.

3 Constraints on the DCDM \rightarrow WDM+DR model

3.1 Presentation of the model

We now turn to a DCDM model¹⁰ where the entirety of the DM sector is considered unstable (*i.e.*, $f_{\text{dcdm}} = 1$ in the language of the first model), decaying into dark radiation and a massive particle, which act as warm dark matter (WDM). As before, we assume the decay products

do not interact with the standard model particles. The DCDM sector is now described by the DCDM lifetime τ , and the fraction ε of rest-mass energy carried away by the massless particle given by $\varepsilon = 1/2 \cdot (1 - m_{\text{wdm}}^2/m_{\text{dcdm}}^2)$, where m_{dcdm} and m_{wdm} are the mother and daughter particle masses respectively. The set of equations describing the evolution of the background energy densities of the dark components reads as follows¹⁰:

$$\dot{\bar{\rho}}_{\text{dcdm}} + 3\mathcal{H}\bar{\rho}_{\text{dcdm}} = -a\Gamma\bar{\rho}_{\text{dcdm}} \quad ; \quad \dot{\bar{\rho}}_{\text{wdm}} + 3(1+w)\mathcal{H}\bar{\rho}_{\text{wdm}} = (1-\varepsilon)a\Gamma\bar{\rho}_{\text{dcdm}} \quad ; \quad (2)$$

$$\dot{\bar{\rho}}_{\text{dr}} + 4\mathcal{H}\bar{\rho}_{\text{dr}} = \varepsilon\Gamma a\bar{\rho}_{\text{dcdm}}, \quad (3)$$

where $w = \bar{P}_{\text{wdm}}/\bar{\rho}_{\text{wdm}}$ is the equation of state of the WDM. In the limit of large τ or small ε , one recovers the Λ CDM model, while setting $\varepsilon = 1/2$ leads to a decay solely into DR.

In the lower panel of Fig. 1, we represent the residuals of the monopole of the galaxy power spectrum for several values of ε and τ to isolate their cosmological effects. In this model, τ – which sets the abundance of the WDM species today – controls the amplitude of the power suppression, while ε controls the cutoff scale from which this suppression occurs (as this parameter sets the free-streaming scale k_{fs}). One can see that the suppression of the galaxy power spectrum increases as τ decreases (as for the previous model), while the suppression starts to occur on larger scales as ε increases. The main difference with the previous model is that the suppression of the power spectrum is no longer due to background effects, but to perturbation effects. At the background level, since one of the daughter particles is massive, the amount of matter can remain roughly equivalent to that of Λ CDM, which allows the model to accommodate Ω_m measurements. At the perturbation level, the presence of the WDM component, which does not cluster on small scales (*i.e.*, when $k > k_{\text{fs}}$), suppresses the galaxy power spectrum.

3.2 EFTofLSS Constraints on the DCDM \rightarrow WDM+DR model

In the right panel of Fig. 2, we display the 1D and 2D posteriors of the reconstructed parameters for the DCDM \rightarrow WDM+DR model with and without the EFTofBOSS dataset, always including a S_8 prior from the KIDS-1000 cosmic shear measurement ($S_8 = 0.759^{+0.024}_{-0.021}$). Interestingly, we can see that this model has the ability to resolve the S_8 tension, and that the inclusion of the EFTofBOSS data does not change this conclusion. With the EFTofBOSS data, we find $\Delta\chi^2 = -3.8$ with respect to the analogous Λ CDM analysis (for 2 extra degrees of freedom) at virtually no cost in χ^2 for other data. In particular, the inclusion of the S_8 prior help in opening up the degeneracy with the DCDM parameters, without degrading the fit to the other data.¹⁰

In addition, one can see in the right panel of Fig. 2 that the main impact of EFTofBOSS data is to cut in the $\log_{10}(\Gamma/\text{Gyr}^{-1}) - \log_{10}(\varepsilon)$ degeneracy, excluding too large values of $\log_{10}(\Gamma/\text{Gyr}^{-1})$. Therefore, the EFTofLSS significantly improves the constraints on the $\tau = \Gamma^{-1}$ parameter at 1σ : $1.61 < \log_{10}(\tau/\text{Gyr}) < 3.71$, to be compared with $1.31 < \log_{10}(\tau/\text{Gyr}) < 3.82$ without the EFTofBOSS data.⁸ Additionally, we observe a notable evolution of the DCDM parameters of the best-fit model compared to the analysis without EFTofBOSS: the best-fit model, with the inclusion of the S_8 likelihood, now has $\Gamma = 0.0083 \text{ Gyr}^{-1}$ ($\tau = 120 \text{ Gyr}$) and $\varepsilon = 0.012$, while previously $\Gamma = 0.023 \text{ Gyr}^{-1}$ ($\tau = 43 \text{ Gyr}$) and $\varepsilon = 0.006$. This means that EFTofBOSS data favors longer lived DM models and therefore a smaller fraction of WDM today $f_{\text{wdm}} \equiv \bar{\rho}_{\text{wdm}}/(\bar{\rho}_{\text{dcdm}} + \bar{\rho}_{\text{wdm}}) \simeq 10\%$ compared to $f_{\text{wdm}} \simeq 27\%$ previously.

Acknowledgments

I am grateful to P. Zhang and G. F. Abellán for their contributions and their kindness. I am also thankful to V. Poulin, my PhD supervisor, for his benevolence and his extremely wise advice.

References

1. Elcio Abdalla et al. Cosmology intertwined: A review of the particle physics, astrophysics, and cosmology associated with the cosmological tensions and anomalies. *JHEAp*, 34:49–211, 2022.
2. N. Aghanim et al. Planck 2018 results. VI. Cosmological parameters. *Astron. Astrophys.*, 641:A6, 2020.
3. Simone Aiola et al. The Atacama Cosmology Telescope: DR4 Maps and Cosmological Parameters. *JCAP*, 12:047, 2020.
4. Marika Asgari et al. KiDS-1000 Cosmology: Cosmic shear constraints and comparison between two point statistics. *Astron. Astrophys.*, 645:A104, 2021.
5. T. M. C. Abbott et al. Dark Energy Survey Year 3 results: Cosmological constraints from galaxy clustering and weak lensing. *Phys. Rev. D*, 105(2):023520, 2022.
6. Chiaki Hikage et al. Cosmology from cosmic shear power spectra with Subaru Hyper Suprime-Cam first-year data. *Publ. Astron. Soc. Jap.*, 71(2):43, 2019.
7. A. Amon et al. Consistent lensing and clustering in a low- S_8 Universe with BOSS, DES Year 3, HSC Year 1 and KiDS-1000. 2 2022.
8. Théo Simon, Guillermo Franco Abellán, Peizhi Du, Vivian Poulin, and Yuhsin Tsai. Constraining decaying dark matter with BOSS data and the effective field theory of large-scale structures. *Phys. Rev. D*, 106(2):023516, 2022.
9. Guillermo Franco Abellán, Riccardo Murgia, Vivian Poulin, and Julien Laval. Implications of the S_8 tension for decaying dark matter with warm decay products. *Phys. Rev. D*, 105(6):063525, 2022.
10. Guillermo Franco Abellán, Riccardo Murgia, and Vivian Poulin. Linear cosmological constraints on two-body decaying dark matter scenarios and the S_8 tension. *Phys. Rev. D*, 104(12):123533, 2021.
11. Benjamin Audren, Julien Lesgourgues, Gianpiero Mangano, Pasquale Dario Serpico, and Thomas Tram. Strongest model-independent bound on the lifetime of Dark Matter. *JCAP*, 12:028, 2014.
12. Kari Enqvist, Seshadri Nadathur, Toyokazu Sekiguchi, and Tomo Takahashi. Decaying dark matter and the tension in σ_8 . *JCAP*, 1509(09):067, 2015.
13. Vivian Poulin, Pasquale D. Serpico, and Julien Lesgourgues. A fresh look at linear cosmological constraints on a decaying dark matter component. *JCAP*, 1608(08):036, 2016.
14. Shohei Aoyama, Toyokazu Sekiguchi, Kiyotomo Ichiki, and Naoshi Sugiyama. Evolution of perturbations and cosmological constraints in decaying dark matter models with arbitrary decay mass products. *JCAP*, 07:021, 2014.
15. S. Alvi, T. Brinckmann, M. Gerbino, M. Lattanzi, and L. Pagano. Do you smell something decaying? Updated linear constraints on decaying dark matter scenarios. 5 2022.
16. Emil Brinch Holm, Thomas Tram, and Steen Hannestad. Decaying warm dark matter revisited. *JCAP*, 08(08):044, 2022.
17. Lea Fuß and Mathias Garny. Decaying Dark Matter and Lyman- α forest constraints. 10 2022.
18. Emil Brinch Holm, Laura Herold, Steen Hannestad, Andreas Nygaard, and Thomas Tram. Discovering a new well: Decaying dark matter with profile likelihoods. 11 2022.
19. Andreas Nygaard, Thomas Tram, and Steen Hannestad. Updated constraints on decaying cold dark matter. *JCAP*, 05:017, 2021.
20. Jozef Bucko, Sambit K. Giri, and Aurel Schneider. Constraining dark matter decays with cosmic microwave background and weak lensing shear observations. 11 2022.
21. John Joseph M. Carrasco, Mark P. Hertzberg, and Leonardo Senatore. The Effective Field Theory of Cosmological Large Scale Structures. *JHEP*, 09:082, 2012.
22. Daniel Baumann, Alberto Nicolis, Leonardo Senatore, and Matias Zaldarriaga. Cosmo-

- logical Non-Linearities as an Effective Fluid. *JCAP*, 07:051, 2012.
23. Rafael A. Porto, Leonardo Senatore, and Matias Zaldarriaga. The Lagrangian-space Effective Field Theory of Large Scale Structures. *JCAP*, 05:022, 2014.
 24. Leonardo Senatore. Bias in the Effective Field Theory of Large Scale Structures. *JCAP*, 1511(11):007, 2015.
 25. Shadab Alam et al. The clustering of galaxies in the completed SDSS-III Baryon Oscillation Spectroscopic Survey: cosmological analysis of the DR12 galaxy sample. *Mon. Not. Roy. Astron. Soc.*, 470(3):2617–2652, 2017.
 26. Beth Reid et al. SDSS-III Baryon Oscillation Spectroscopic Survey Data Release 12: galaxy target selection and large scale structure catalogues. *Mon. Not. Roy. Astron. Soc.*, 455(2):1553–1573, 2016.
 27. Théo Simon, Pierre Zhang, Vivian Poulin, and Tristan L. Smith. On the consistency of effective field theory analyses of BOSS power spectrum. 8 2022.
 28. Guido D’Amico, Jérôme Gleyzes, Nickolas Kokron, Katarina Markovic, Leonardo Senatore, Pierre Zhang, Florian Beutler, and Héctor Gil-Marín. The Cosmological Analysis of the SDSS/BOSS data from the Effective Field Theory of Large-Scale Structure. *JCAP*, 05:005, 2020.
 29. Mikhail M. Ivanov, Marko Simonović, and Matias Zaldarriaga. Cosmological Parameters from the BOSS Galaxy Power Spectrum. 2019.
 30. Thomas Colas, Guido D’Amico, Leonardo Senatore, Pierre Zhang, and Florian Beutler. Efficient Cosmological Analysis of the SDSS/BOSS data from the Effective Field Theory of Large-Scale Structure. *JCAP*, 06:001, 2020.
 31. Oliver H. E. Philcox, Mikhail M. Ivanov, Marko Simonović, and Matias Zaldarriaga. Combining Full-Shape and BAO Analyses of Galaxy Power Spectra: A 1.6% CMB-independent constraint on H_0 . 2020.
 32. Shi-Fan Chen, Zvonimir Vlah, and Martin White. A new analysis of galaxy 2-point functions in the BOSS survey, including full-shape information and post-reconstruction BAO. *JCAP*, 02(02):008, 2022.
 33. Pierre Zhang, Guido D’Amico, Leonardo Senatore, Cheng Zhao, and Yifu Cai. BOSS Correlation Function analysis from the Effective Field Theory of Large-Scale Structure. *JCAP*, 02(02):036, 2022.
 34. Shi-Fan Chen, Martin White, Joseph DeRose, and Nickolas Kokron. Cosmological analysis of three-dimensional BOSS galaxy clustering and Planck CMB lensing cross correlations via Lagrangian perturbation theory. *JCAP*, 07(07):041, 2022.
 35. Théo Simon, Pierre Zhang, and Vivian Poulin. Cosmological inference from the EFTofLSS: the eBOSS QSO full-shape analysis. 10 2022.
 36. Tristan L. Smith, Vivian Poulin, and Théo Simon. Assessing the robustness of sound horizon-free determinations of the Hubble constant. 8 2022.
 37. Mikhail M. Ivanov, Marko Simonović, and Matias Zaldarriaga. Cosmological Parameters and Neutrino Masses from the Final Planck and Full-Shape BOSS Data. *Phys. Rev. D*, 101(8):083504, 2020.
 38. Suresh Kumar, Rafael C. Nunes, and Priya Yadav. Updating non-standard neutrinos properties with Planck-CMB data and full-shape analysis of BOSS and eBOSS galaxies. 5 2022.
 39. Guido D’Amico, Leonardo Senatore, and Pierre Zhang. Limits on w CDM from the EFTofLSS with the PyBird code. *JCAP*, 01:006, 2021.
 40. Guido D’Amico, Yaniv Donath, Leonardo Senatore, and Pierre Zhang. Limits on Clustering and Smooth Quintessence from the EFTofLSS. 12 2020.
 41. Pedro Carrilho, Chiara Moretti, and Alkistis Pourtsidou. Cosmology with the EFTofLSS and BOSS: dark energy constraints and a note on priors. 7 2022.
 42. Anton Chudaykin, Konstantin Dolgikh, and Mikhail M. Ivanov. Constraints on the cur-

- vature of the Universe and dynamical dark energy from the Full-shape and BAO data. *Phys. Rev. D*, 103(2):023507, 2021.
43. Aaron Glanville, Cullan Howlett, and Tamara M. Davis. Full-Shape Galaxy Power Spectra and the Curvature Tension. 5 2022.
 44. Guido D’Amico, Leonardo Senatore, Pierre Zhang, and Henry Zheng. The Hubble Tension in Light of the Full-Shape Analysis of Large-Scale Structure Data. *JCAP*, 05:072, 2021.
 45. Mikhail M. Ivanov, Evan McDonough, J. Colin Hill, Marko Simonović, Michael W. Toomey, Stephon Alexander, and Matias Zaldarriaga. Constraining Early Dark Energy with Large-Scale Structure. *Phys. Rev. D*, 102(10):103502, 2020.
 46. Florian Niedermann and Martin S. Sloth. New Early Dark Energy is compatible with current LSS data. *Phys. Rev. D*, 103(10):103537, 2021.
 47. Théo Simon, Pierre Zhang, Vivian Poulin, and Tristan L. Smith. Updated constraints from the effective field theory analysis of BOSS power spectrum on Early Dark Energy. 8 2022.
 48. Henrique Rubira, Asmaa Mazoun, and Mathias Garny. Full-shape BOSS constraints on dark matter interacting with dark radiation and lifting the S_8 tension. 9 2022.
 49. Rafael C. Nunes, Sunny Vagnozzi, Suresh Kumar, Eleonora Di Valentino, and Olga Mena. New tests of dark sector interactions from the full-shape galaxy power spectrum. *Phys. Rev. D*, 105(12):123506, 2022.
 50. Alex Laguë, J. Richard Bond, Renée Hložek, Keir K. Rogers, David J. E. Marsh, and Daniel Grin. Constraining Ultralight Axions with Galaxy Surveys. 4 2021.
 51. D. M. Scolnic et al. The Complete Light-curve Sample of Spectroscopically Confirmed SNe Ia from Pan-STARRS1 and Cosmological Constraints from the Combined Pantheon Sample. *Astrophys. J.*, 859(2):101, 2018.
 52. Florian Beutler, Chris Blake, Matthew Colless, D. Heath Jones, Lister Staveley-Smith, Lachlan Campbell, Quentin Parker, Will Saunders, and Fred Watson. The 6dF Galaxy Survey: Baryon Acoustic Oscillations and the Local Hubble Constant. *Mon. Not. Roy. Astron. Soc.*, 416:3017–3032, 2011.
 53. Ashley J. Ross, Lado Samushia, Cullan Howlett, Will J. Percival, Angela Burden, and Marc Manera. The clustering of the SDSS DR7 main Galaxy sample – I. A 4 per cent distance measure at $z = 0.15$. *Mon. Not. Roy. Astron. Soc.*, 449(1):835–847, 2015.
 54. Shadab Alam et al. The clustering of galaxies in the completed SDSS-III Baryon Oscillation Spectroscopic Survey: cosmological analysis of the DR12 galaxy sample. *Mon. Not. Roy. Astron. Soc.*, 470(3):2617–2652, 2017.
 55. Victoria de Sainte Agathe et al. Baryon acoustic oscillations at $z = 2.34$ from the correlations of $\text{Ly}\alpha$ absorption in eBOSS DR14. *Astron. Astrophys.*, 629:A85, 2019.